Attachment 26

LR-N06-0286
LCR H05-01, Rev. 1

HOPE CREEK GENERATING STATION
FACILITY OPERATING LICENSE NPF-57
DOCKET NO. 50-354

REQUEST FOR LICENSE AMENDMENT
EXTENDED POWER UPRATE

Estimating High Frequency Flow Induced Vibration in the Main Steam Lines at Hope Creek Unit 1: A Subscale Four Line Investigation of Standpipe Behavior
CDI Report No. 06-16NP
September 2006

This Report Does Not Contain Continuum Dynamics, Inc. Proprietary Information

C.D.I. Report No. 06-16NP

Estimating High Frequency Flow Induced Vibration in the Main Steam Lines at Hope Creek Unit 1: A Subscale Four Line Investigation of Standpipe Behavior

Revision 1

Prepared by

Continuum Dynamics, Inc.
34 Lexington Avenue
Ewing, NJ 08618

Prepared under Purchase Order No. 4500341046 for

Nuclear Business Unit, PSEG Nuclear LLC
Materials Center, Alloway Creek Neck Road
Hancocks Bridge, NJ 08038

Approved by

Alan J. Bilanin

Reviewed by

Milton E. Teske

September 2006

Executive Summary

As part of the engineering effort in support of power uprate at Hope Creek Unit 1, Continuum Dynamics, Inc. undertook a subscale examination of the standpipe/valve geometry on two of the four main steam lines (one at a time), in an effort to validate the frequency onset at which flow induced vibration, resulting from standpipe/valve flow resonance, could potentially impact steam dryer loads. In this study Continuum Dynamics, Inc. constructed a nominal one-sixth scale model of main steam lines A and D at Hope Creek Unit 1, from the steam dome to beyond the standpipes, then tested the as-built configuration of standpipes and Target Rock valves. The findings suggested that the as-built configuration, at EPU conditions, will be past excitation onset, and that this loading should receive further evaluation, and possible mitigation.

As part of a follow-on effort, Continuum Dynamics, Inc. constructed a nominal one-eighth scale model of the complete steam line system at Hope Creek Unit 1, from the steam dome to the turbine, with the objective of determining whether the existing standpipes have an acceptable level of excitation. In addition, a modified configuration was tested, with a standpipe height reduction of five inches full scale. The findings suggest that the level of excitation at CLTP conditions are marginally maintained at EPU conditions with the shortened standpipes.

This effort provides PSEG with a subscale test that quantifies the level of excitation to be expected at Hope Creek Unit 1 at EPU conditions.

Table of Contents

1. Introduction

As part of its effort in support of power uprate at Hope Creek Unit 1 (HC1), PSEG Nuclear LLC contracted with Continuum Dynamics, Inc. (C.D.I.) to evaluate existing main steam line data (collected downstream of the standpipes) to estimate the pressure loads expected on the steam dryer at Current Licensed Thermal Power (CLTP). These results [1], coupled with a finite element analysis of the resulting loads [2], suggested that the steam dryer stresses are acceptable at CLTP conditions. To go to higher power levels (EPU), PSEG requested that C.D.I. evaluate the potential for flow induced vibration (FIV) in the main steam lines as a result of resonance of the as-built standpipe/valve combination. Studies conducted by Exelon for Quad Cities Unit 1 and Unit 2 suggested that excitation of the standpipe/valve should be explored, as this mechanism was most responsible for the pressure loading experienced on the Quad Cities steam dryers [3].

Such a study was undertaken for Hope Creek [4], and suggested that the as-built configuration, at EPU conditions, would be past excitation onset, and that this loading should receive further evaluation, and possible mitigation.

The frequencies associated with FIV are known to correspond to a resonance associated with the inlet standpipes connected to safety valves, and have been the source of problems in several power plants in recent years [5–8]. Specifically, in [8], C.D.I. conducted a series of tests in support of damage observed on Columbia's main steam line safety valves. These tests concluded that the geometry of the Columbia standpipes and safety valve inlets, with flow conditions of approximately 60% to 70% of licensed power, resulted in a resonance at approximately 1050 Hz in a scaled facility (corresponding to approximately 204 Hz in the plant). The observation was made that properly scaled tests could provide data that could be used for design.

At the request of PSEG, C.D.I. applied the insights gained from the study on Columbia, and previous work for Exelon, to the HC1 standpipe/valve configuration. This report summarizes the test results on a scale model of the HC1 plant with four main steam lines.

2. Objectives

Construction of a high Reynolds number subscale test facility, simulating the steam delivery system of HC1, was done so as to achieve the following goals:

1. Measure the excitation frequency and amplitudes of the as-built standpipe/valve configuration (encompassing all four main steam lines) at HC1, as a function of entrance Mach number, and determine the behavior of the system at CLTP and EPU conditions.

2. Compare this behavior to the measured excitation frequency and amplitudes of the shortened standpipe configuration.

3. Theoretical Approach

A 1/8th test facility is proposed as a means of measuring the effect of standpipes on the anticipated acoustic signal to the steam dome. A description of the phenomenon at work, analytical tools to be used, and scaling laws justifying the subscale tests are given here.

3.1 Side Branch Excitation Mechanism

The phenomenon of flow-excited acoustic resonance of closed side branches has been examined for many years (see as early as [9] and [10]). In this situation acoustic resonance of the side branch is caused by feedback from the acoustic velocity of the resonant standing wave in the side branch itself. Figure 3.1 illustrates the typical geometry used here and in the standpipes at HC1. The main steam line flow velocity U approaches an open side branch of diameter d and length L. Pressure p as a function of time t can be measured at the closed end of the pipe. The flow velocity induces perturbations in the shear layer at the upstream separation location in the main steam line. As these perturbations are amplified and convected downstream, they interact with the acoustic field and produce acoustic energy which reinforces the resonance of the acoustic mode. Ziada has studied this effect extensively [11–13], and has shown that the flow velocity of first onset of instability U_{on} corresponds to a typical Strouhal number of St = 0.55, where St is defined as

$$St = \frac{f(d+r)}{U_{on}} \tag{3.1}$$

where d is the diameter of the standpipe, r is the radius of the inlet chamfer, and f is the first mode of acoustic oscillation in the pipe system. A design chart that more accurately infers St, based on d and the diameter D of the main steam line, may be found in [11].

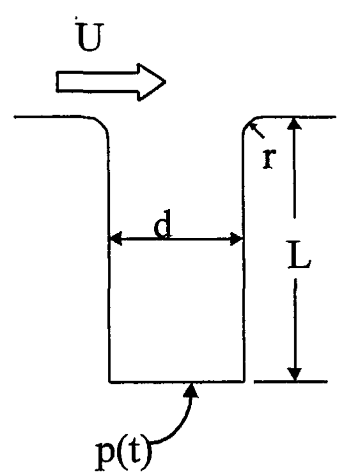

Figure 3.1. Schematic of the side branch geometry.

Solving for U_{on} in Equation 3.1, it may be seen that the onset velocity is linearly proportional to the standpipe diameter, so long as that diameter does not change the first acoustic mode frequency of the standpipe.

The implications of this side branch excitation frequency may be seen by examining the behavior of the pressure response as a function of Strouhal number St (Figure 3.2). For large Strouhal numbers (beginning on the right side of the figure), the RMS pressure p_{RMS} begins increasing (at a specific onset Strouhal number and flow velocity U_{on}, depending on acoustic speed a, pipe diameter d, and pipe length L), reaches a peak value, then decreases. Flow velocity increases from right to left in this figure, where it may then be seen that this phenomenon – if it occurs in a standpipe/valve configuration – will occur at a low power level, reach a peak effect, then diminish and disappear at sufficiently high power levels.

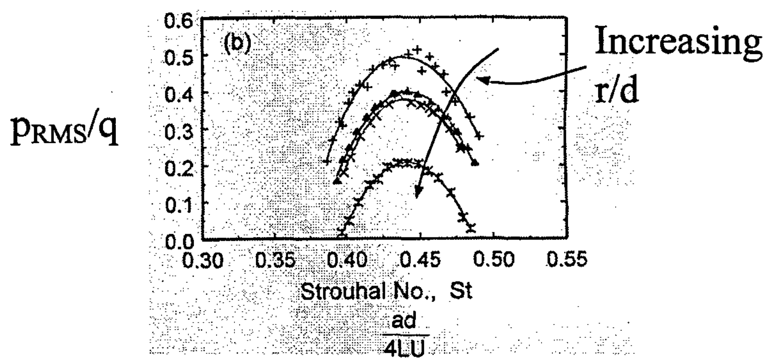

Figure 3.2. Strouhal number behavior, where q is the dynamic pressure ($\frac{1}{2}\rho U^2$), ρ is the fluid density, and a is the acoustic speed [14].

Initially, it may be anticipated that the first mode frequency f_1 can be approximated by the quarter-standing wave frequency of the standpipe/valve combination

$$f_1 = \frac{a}{4L} \qquad (3.2)$$

Since the standpipe/valve combination changes area as a function of distance from the main steam line to the valve disk, a more accurate estimate of f_1 may be generated by including these area change effects. The combination of an accurate excitation frequency f_1 and subsequent calculation of onset velocity U_{on} with the appropriate Strouhal number then characterizes the behavior of the standpipe/valve combination considered.

3.2 Scaling Laws

[[

(3)]]

[[

(3)]]

[[

3)]]

4. Test Approach

The purpose of the testing effort is to measure the excitation frequency and amplitudes of the as-built and shortened standpipe/valve configurations, and determine their behavior at CLTP and EPU conditions. To do so, a one-eighth scaled test facility was constructed that represents the HC1 steam delivery system.

4.1 Test Design

[[

(3)]]

[[

(3)]]

The standpipe locations at HC1 are summarized in Table 4.1. Main steam line drawings and all necessary details were provided by PSEG in [16].

Table 4.1. Standpipe location summary at HC1.

Main Steam Line	Valve Type	Distance From Upstream Elbow (ft)
A	Target Rock	5.13
A	Target Rock	8.14
A	Target Rock	11.16
B	Target Rock	6.95
B	Target Rock	10.11
B	Target Rock	17.90
B	Blind Flange	21.06
B	Target Rock	24.21
C	Target Rock	6.95
C	Target Rock	10.07
C	Target Rock	17.86
C	Target Rock	24.17
D	Target Rock	5.09
D	Target Rock	8.15
D	Target Rock	11.17

From drawings, pictures, and additional information supplied by PSEG [16], an approximate cross-sectional area of each standpipe/valve configuration – as a function of distance from the main steam line – was generated. These cross-sectional areas include the standpipe length and diameter, mating flange to the valve, and internal valve geometries to the closed end of the valve. The configurations tested are shown in Appendix A.

[[

[3]]]

Figure 4.2. Subscale dryer schematic.

[[

(3)]]

Figure 4.3a. The four MSLs from the steam dome to past the standpipes. Note the standpipes.

[[

(3)]]

Figure 4.3b. The four MSLs from the steam dome to past the "D" ring. The four lines off the right side of the picture should actually be down (the whole piping system is on its side). The pipe in front is from the $1/5^{th}$ scale test.

[[

(3)]]

Figure 4.3c. Detail at the "D" ring.

[[

(3)]]

Figure 4.3d. Turbine end of MSLs – the tank is the accumulator for the 1/5th scale test rig. The closer valves are opened simultaneously to initiate the test. The far valves (at the corner of the piping on the right center of the picture) are the control valves and were set to 15 degrees closed, consistent with the Quad Cities work.

5. Test Apparatus and Instrumentation

Test apparatus for the PSEG 1/8th scale test program consists of a pressure tank, a system of pipes to model full scale steam lines, two sets of interchangeable model pressure relief valves, four ball valves, and a set of interchangeable orifices.

5.1 Experimental Facility

[[

[(3)]]

[[

(3)]]

Table 5.1. Plant power and main steam line Mach numbers, where the CLTP Mach number = 0.0913 and the EPU (1.15 x CLTP) Mach number = 0.1050.

[[

(3)]]

[[

____ (3)]]

Figure 5.2. Schematic of data acquisition system with ten DP transducers.

6. Test Matrix

Table 6.1. Hope Creek Unit 1 Four-Line Test Matrix.

[[

(3)]]

Table 6.1. Hope Creek Unit 1 Four-Line Test Matrix (continued).

[[

[3]]]

7. Test Procedure

7.1 Data Collection

[[

(3)]]

7.2 Data Reduction

[[

(3)]]

[[

[3]]]

Figure 7.1. Stagnation pressure time history.

8. Results and Discussion

The purpose of the PSEG subscale test program was to characterize the behavior of the standpipe/valves currently at HC1, and to determine the effect of shortening the standpipes. It would be desirable if the shortened standpipe were to result in pressure oscillations at EPU conditions that were lower than the as-built pressure oscillations at CLTP conditions.

It should be noted that, overall, the 56 tests summarized previously in Table 6.1 can be divided into four general areas of investigation:

1. Tests hc2-1 to hc2-6 served to shakedown the piping system.

2. Tests hc2-7 to hc2-15 developed the statistics needed to characterize the behavior of the Mach number, from the entrance to the orifice (Figure 5.1). [[

   (3)]]

3. Tests hc2-16 to hc2-36 examined the behavior of the as-built configuration for all Mach numbers tested.

4. Tests hc2-37 to hc2-56 examined the behavior of the shortened standpipe configuration for all Mach numbers tested.

The results of the test program may be examined with regard to excitation frequency and RMS pressure as a function of power level, comparison of PSDs, and predicted peak pressures on the steam dryer. Of these, the change in peak pressures on the steam dryer provides the best extrapolation of the potential impact on steam dryer stresses.

8.1 Excitation Frequency

[[

(3)]]

Table 8.1. Comparison between predicted and measured excitation frequencies for HC1.

[[

(3)]]

8.2 Mach Number Effect / Plant Power Level

The subscale tests swept Mach number by changing orifice size (increasing orifice size to increase Mach number). The effect of Mach number is not easily seen from a review of the PSDs of measured pressure (found in Appendix B). However, the task is simplified by noting that the largest contribution to the RMS is the discrete frequency peaks attributed to the excitation of valve standpipes. Figures 8.1 to 8.5 plot the normalized RMS pressures at the ten pressure transducers as a function of Mach number (plant power level). RMS pressures include the signal from 600 to 900 Hz.

Referring to these figures, it should be noted that the black solid circles represent the data taken with the as-built configuration, while the red solid circles represent the data taken with the shortened standpipe configuration. Every Mach number was repeated, and except for an outlier in Figure 8.3 for PD6, the test pairs appear reproducible. The curves shown on these figures are cubic curve fits to the data. RMS pressures include only the signal from 600 to 900 Hz to better demonstrate the change due to SRV excitation.

[[

(3)]]

[[

(3)]]

Figure 8.1. Normalized RMS Pressure on main steam line A. PD1: upstream pressure transducer; PD2: downstream pressure transducer. Black = as-built; red = shortened standpipe.

[[

(3)]]

Figure 8.2. Normalized RMS Pressure on main steam line B. PD3: upstream pressure transducer; PD4: downstream pressure transducer. Black = as-built; red = shortened standpipe.

[[

(3)]]

Figure 8.3. Normalized RMS Pressure on main steam line C. PD5: upstream pressure transducer; PD6: downstream pressure transducer. Black = as-built; red = shortened standpipe.

[[

(3)]]

Figure 8.4. Normalized RMS Pressure on main steam line D. PD7: upstream pressure transducer; PD8: downstream pressure transducer. Black = as-built; red = shortened standpipe.

[[

(3)]]

Figure 8.5. Normalized RMS Pressure at the dryer pressure transducers. PD9: opposite main steam line A; PD10: opposite main steam line D. Black = as-built; red = shortened standpipe.

Table 8.2. RMS pressure summary of 1/8th scale tests (600 to 900 Hz only).

[[

(3)]]

8.3 Comparisons of PSDs

All data obtained have been reduced to PSDs of the pressure, where the pressures have been normalized by CLTP main steam line dynamic pressure. This allows comparison between normalized PSDs so that data can be compared directly. Appendix B contains these PSD plots for all collected data.

For example, Figure 8.6 reproduces the hc2-23 results on the dryer for the as-built configuration as CLTP conditions, while Figure 8.7 reproduces the hc2-19 results on the dryer at EPU conditions. It may be seen that the PSD peak levels are increased approximately 250% between the two power levels.

Similar comparisons can be made with all the data in Appendix B.

8.4 Steam Dryer Loads from the Acoustic Circuit Model

Comparing pressure time histories at discrete locations in the steam delivery system is complicated by the fact that the measured pressure is both a function of source amplitude and frequency. The fact that the standpipe changes change both amplitude and frequency of the standpipe resonator (source) suggests that it might be easier to understand the level of mitigation by computing the differential pressure loads at selected nodal locations on the steam dryer. Figure 8.8 plots the low resolution results for peak normalized differential pressures across the steam dryer, comparing CLTP conditions as-built with EPU conditions as-built. The non-physical 80 Hz signal has been removed from these results [20]. Rev 1 Rev 1

[[

(3)]]

Figure 8.6. Normalized PSD for Test hc2-23: as-built configuration at a Mach number = CLTP. Dryer A: steam dryer pressure transducer location opposite MSL A; Dryer D: steam dryer pressure transducer location opposite MSL D.

[[

(3)]]

Figure 8.7. Normalized PSD for Test hc2-19: as-built configuration at a Mach number = 1.15 × CLTP. Dryer A: steam dryer pressure transducer location opposite MSL A; Dryer D: steam dryer pressure transducer location opposite MSL D.

[[

Rev 1

$^{(3)}$]]

Figure 8.8. Dryer peak differential pressure loads computed on the 1/8th scale steam dryer using the Bounding Pressure Methodology acoustic circuit model [21].

[[

Rev 1

$^{(3)}$]]

9. Conclusions

One-eighth scale tests measured the excitation frequency and amplitudes of the as-built standpipe/valve configuration (encompassing all four main steam lines) at HC1, as a function of entrance Mach number, and determined the behavior of the system at CLTP and EPU conditions. [[

Rev 1

(3)]]

10. References

1. Continuum Dynamics, Inc. 2005. Hydrodynamic Loads on Hope Creek Unit 1 Steam Dryer to 200 Hz. C.D.I. Report No. 05-17.

2. Continuum Dynamics, Inc. 2005. Stress Analysis of the Hope Creek Unit 1 Steam Dryer for CLTP. C.D.I. Report No. 05-25.

3. Continuum Dynamics, Inc. 2005. Evaluation of Continuum Dynamics, Inc. Steam Dryer Load Methodology Against Quad Cities Unit 2 In-Plant Data. C.D.I. Report No. 05-10.

4. Continuum Dynamics, Inc. 2005. Onset of High Frequency Flow Induced Vibration in the Main Steam Lines at Hope Creek Unit 1: A Subscale Investigation of Standpipe Behavior. C.D.I. Report No. 05-31.

5. Webb, M. and P. Ellenberger. 1995. Piping Retrofit Reduces Valve-Damaging Flow Vibration. *Power Engineering*.

6. Bernstein, M. D. and Bloomfield, W. J. 1989. Malfunction of Safety Valves Due to Flow Induced Vibration. *Flow-Induced Vibrations 1989* (ed: M. K. Au-Yang, S. S. Chen, S. Kaneko and R. Chilukuri) PVP 154: 155-164. New York: ASME.

7. Coffman, J. T. and Bernstein, M. D. 1980. Failure of Safety Valves Due to Flow Induced Vibration. *Transactions of the ASME* 102.

8. Continuum Dynamics, Inc. 2002. Mechanisms Resulting in Leakage from Main Steam Safety Valves. C.D.I. Technical Note No. 02-16.

9. Chen, Y. N. and D. Florjancic. 1975. Vortex-Induced Resonance in a Pipe System due to Branching. *Proceedings of International Conference on Vibration and Noise in Pump, Fan and Compressor Installations* 79-86. University of Southampton, England.

10. Baldwin, R. M. and H. R. Simmons. 1986. Flow-Induced Vibration in Safety Relief Valves. *ASME Journal of Pressure Vessel Technology* 108: 267-272.

11. Ziada, S. and Shine, S. 1999. Strouhal Numbers of Flow-Excited Acoustic Resonance of Closed Side Branches. *Journal of Fluids and Structures* 13: 127-142.

12. Ziada, S. 1994. A Flow Visualization Study of Flow Acoustic Coupling at the Mouth of a Resonant Side-Branch. *Journals of Fluids and Structures* 8: 391-416.

13. Graf, H. R. and S. Ziada. 1992. Flow-Induced Acoustic Resonance in Closed Side Branches: An Experimental Determination of the Excitation Source. *Proceedings of ASME International Symposium on Flow-Induced Vibration and Noise, Vol. 7: Fundamental Aspects of Fluid-Structure Interactions* (ed: M. P. Paidoussis, T. Akylas and P. B. Abraham). AMD-Vol. 51: 63-80. New York: ASME.

14. Weaver, D. S. and MacLeon, G. O. 1999. Entrance Port Rounding Effects on Acoustic Resonance in Safety Relief Valves. PVP-Vol. 389, Flow Induced Vibration- ASME 1999.

15. Continuum Dynamics, Inc. 2004. Plant Unique Steam Dryer Loads to Support I&E Guidelines. C.D.I. Technical Memo No. 04-14.

16. PSEG VTD Drawing No. PN1-G0001-0020, Primary Steam Piping, Sheets 001 Rev. 8, 002 Rev. 8, and 003 Rev. 8 (GE Drawing No. 761E468). PSEG VTD Drawing No. PN1-G0001-0060, Expander Flange Rev. 8 (GE Drawing No. 131C7672). PSEG Vendor Manual PN1-B21-F013-0162, Rev. 8, Target Rock Relief Valve 7567F (dimensions are provided in Figure 4 of the manual; some dimensions are scaled off the drawing). Bonney Forge Drawing No. DFA-17-009, Typical Sweepolet cross-section (some dimensions are scaled off the drawing). PSEG Drawings No. PN-B11-D041-66, PN1-B11-2010-0079, FSK-P-214, FSK-P-215, 1-P-AB-01, 1-P-AB-011, 1-P-AB-001, 1-P-AB-002, 1-P-AB-003, 1-P-AB-004, FSK-P-223, and 1-P-AB-023.

17. Shapiro, A. H. 1953. The Dynamics and Thermodynamics of Compressible Fluid Flow. Volume I. John Wiley and Sons: New York, NY.

18. Kayser, J. C. and R. L. Shambaugh. 1991. Discharge Coefficients for Compressible Flow Through Small-Diameter Orifices and Convergent Nozzles. *Chemical Engineering Science* 46:1697-1711.

19. Continuum Dynamics, Inc. 2006. Mitigation of Pressure Oscillations in the Quad Cities Unit 2 Steam Delivery System: A Subscale Four Main Steam Line Investigation of Standpipe Behavior. C.D.I. Report No. 06-08.

20. Continuum Dynamics, Inc. 2006. High and Low Frequency Steam Dryer Loads by Acoustic Circuit Methodology. C.D.I. Technical Memorandum No. 06-25P. Rev 1

21. Continuum Dynamics, Inc. 2005. Bounding Methodology to Predict Full Scale Steam Dryer Loads from In-Plant Measurements. C.D.I. Technical Note No. 05-28P.

Appendix A: Standpipe/Valve Cross-Sections

This appendix contains schematics of the as-built standpipe/valve configuration and the shortened standpipe configuration at nominal $1/8^{th}$ scale. All dimensions are in inches.

[[

(3)]]

Figure A.1. [[

(3)]]

[[

$^{(3)}$]]

Figure A.2. [[

$^{(3)}$]]

Appendix B: Mitigation PSD Results

Appendix B provides the normalized PSDs for the as-built and shortened standpipe tests. Here, normalized PSD is obtained by normalizing the pressure trace by the dynamic pressure at CLTP, then constructing the PSD from the Fast Fourier transform.

The test matrix is found in Table 6.1. The transducer designations are as follows:

Pressure Transducer Designations

PD1	MSL A upstream strain gage location
PD2	MSL A downstream strain gage location
PD3	MSL B upstream strain gage location
PD4	MSL B downstream strain gage location
PD5	MSL C upstream strain gage location
PD6	MSL C downstream strain gage location
PD7	MSL D upstream strain gage location
PD8	MSL D downstream strain gage location
PD9	Steam dryer location opposite MSL A
PD10	Steam dryer location opposite MSL D

[[

(3)]]

[[

(3)]]

[[

____(3)]]

[[

(3)]]

[[

(3)]]

[[

(3)]]

[[

(3)]]

[[

(3)]]

[[

(3)]]

[[

(3)]]

[[

[3]]]

[[

(3)]]

[[

---

[3]]]

[[

____ (3)]]

[[

(3)]]

[[

(3)]]

[[

(3)]]

[[

(3)]]

[[

(3)]]

[[

(3)]]

[[

(3)]]

[[

(3)]]

[[

[(3)]]]

[[

[3]]]

[[

[(3)]]

[[

(3)]]

[[

(3)]]

[[

(3)]]

[[

[(3)]]

[[

(3)]]

[[

(3)]]

[[

(3)]]

[[

[(3)]]]

[[

(3)]]

[[

(3)]]

[[

(3)]]

[[

[(3)]]]

[[

(3)]]

[[

[3]]]

[[

(3)]]

[[

(3)]]

[[

[(3)]]]

[[

(3)]]

[[

(3)]]

[[

(3)]]

[[

(3)]]

[[

[3]]]

[[

(3)]]

[[

(3)]]

[[

(3)]]

[[

(3)]]

[[

(3)]]

[[

(3)]]

[[

[3]]]

[[

(3)]]

[[

(3)]]

[[

[(3)]]]

[[

(3)]]

[[

(3)]]

[[

(3)]]

[[

(3)]]

[[

(3)]]

[[

(3)]]

[[

(3)]]

[[

(3)]]

[[

(3)]]

[[

[3]]]

[[

(3)]]

[[

(3)]]

[[

(3)]]

[[

(3)]]

[[

(3)]]

[[

[(3)]]]

[[

[3]]]

[[

[3]]]

[[

(3)]]

[[

(3)]]

[[

(3)]]

[[

[3]]]

[[

(3)]]

[[

[3]]]

[[

(3)]]

[[

(3)]]

[[

(3)]]

[[

(3)]]

[[

[3]]]

[[

(3)]]

[[

(3)]]

[[

(3)]]

[[

[3]]]

[[

[3]]]

[[

(3)]]

[[

[(3)]]]

[[

(3)]]

[[

(3)]]

[[

____ (3)]]

[[

____ [(3)]]]

[[

(3)]]

[[

[3]]]

[[

(3)]]